

A DFT and AIM Study of the Proline-Catalyzed Asymmetric Cross-Aldol Addition of Acetone to Isatins: A Rationalization for the Reversal of Chirality

Rodrigo J. Corrêa,^[a] Simon J. Garden,^{*[a]} Gaetano Angelici,^[b] and Claudia Tomasini^{*[b]}

Keywords: Asymmetric catalysis / Organocatalysis / Proline / Isatin / Density functional calculations / Atoms in molecules

The steric and stereoelectronic effects that control the enantioselectivity in the cross-aldol addition of acetone to isatin catalyzed by L-proline have been studied by means of DFT and AIM calculations. This reaction results in a reversal of enantioselectivity compared with the corresponding cross-aldol addition to 4,6-dibromoisatin and aldehydes. DFT calculations of the cross-aldol transition states indicate that product formation follows different pathways for the substrates isatin and 4,6-dibromoisatin. In the case of isatin, the *S* enantiomer is favoured as a consequence of a stereoelec-

tronic effect that results in a lower-energy transition state for the *S* enantiomer relative to the *R* enantiomer. In contrast, the cross-aldol addition of acetone to 4,6-dibromoisatin furnishes the expected *R* enantiomer owing to a steric effect of the 4-bromo substituent which inhibits the formation of the *S* enantiomer via the stereoelectronically favoured transition state.

(© Wiley-VCH Verlag GmbH & Co. KGaA, 69451 Weinheim, Germany, 2008)

Introduction

The cross-aldol addition of acetone to isatins has been recently studied^[1] and results in the synthesis of a quaternary stereocentre with good enantioselectivity.^[2] This reaction can be used for the synthesis of interesting compounds belonging to the family of convolutamydines, natural products previously isolated from the Floridian marine bryozoan, *Amathia convoluta*, that display interesting antitumour activity.^[3]

Recently, we described the first enantioselective synthesis of convolutamydine A by the cross-aldol addition of acetone to 4,6-dibromoisatin (**1**).^[1a] This reaction was previously studied by using the model compound isatin (**2**) in which the two bromines in the 4- and 6-positions of the phenyl ring are absent.^[1b] The formation of the new stereogenic centre was catalyzed by proline or by prolinamides, with large enantiomeric excesses being obtained when prolinamides were employed. Enantiomerically pure compounds were obtained after chromatography and crystallization and their absolute configurations were unambiguously established by X-ray diffraction. When the cross-aldol addition of acetone to isatin was catalyzed by L-proline, the enantio-

meric excess was always poor and the product had the opposite chirality to that expected based upon literature models.^[4] In contrast, the expected configuration was obtained for the cross-aldol addition of acetone to 4,6-dibromoisatin.^[1a] Thus the mechanism of this interesting reaction has been investigated in more depth by using DFT and AIM calculations to interpret the experimental results.

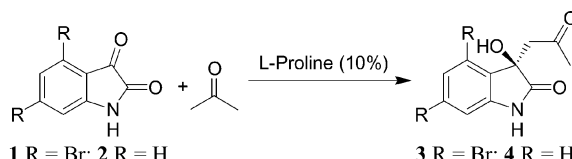
Results and Discussion

To verify whether or not the inversion of configuration observed in the products of the cross-aldol reaction of isatin and 4,6-dibromoisatin should be ascribed only to the presence of the 4-bromo substituent, we performed the L-proline-catalyzed cross-aldol addition of acetone to isatin and 4,6-dibromoisatin under the same reaction conditions. The absolute configurations of the products were assigned by comparison of the HPLC retention times of the reaction products with those whose absolute configurations were determined by single-crystal X-ray diffraction. Table 1 reports the chemical yields and enantiomeric excesses of the cross-aldol reactions.

The reaction between acetone and isatin (**2**) was performed at three different temperatures (entries 1–3) and revealed a small temperature effect on the enantiomeric excess. The *S* enantiomer was always favoured. This result contrasts that generally observed in the aldol addition of acetone to aldehydes when catalyzed by proline or prolinamides.^[4] In contrast, the cross-aldol reaction of 4,6-dibromoisatin (**4**) and acetone (entries 4–6) revealed a stronger temperature effect: at room temperature the reaction afforded a racemic mixture, whilst at –15 °C the *R* enantiomer

[a] Instituto de Química, Departamento de Química Orgânica, Universidade Federal do Rio de Janeiro, Ilha do Fundão, Bloco A, CT, CEP 219450-900, Rio de Janeiro, Brazil
Fax: +55-21-25627256
E-mail: garden@iq.ufrj.br

[b] Dipartimento di Chimica “G. Ciamician” – Alma Mater Studiorum Università di Bologna, Via Selmi 2, 40126 Bologna, Italy
Fax: +39-0512099456
E-mail: claudia.tomasini@unibo.it

Table 1. Enantiomeric excesses and yields of the aldol reactions of isatin and 4,6-dibromoisatin with acetone catalyzed by L-proline.^[a]


Entry	R	Time [h]	Temp. [°C]	% Yield	% ee ^[b]	Configuration ^[c]
1	H	17	20	quant.	25	<i>S</i>
2	H	17	-15	quant.	37	<i>S</i>
3	H	17	-30	42	27	<i>S</i>
4	Br	17	20	quant.	3.5	<i>S</i>
5	Br	17	-15	86	55	<i>R</i>
6	Br	17	-30	0	—	—

[a] The concentration of isatin in acetone was 0.15 M and 10 mol-% of the catalyst was used. [b] ee values were determined by HPLC [conditions: (i) for R = H: solvent: hexane/2-propanol, 80:20; flow: 0.9 mL/min; column: AD Diacel; retention times, *S*: 11.66 min, *R*: 15.28 min; (ii) for R = Br: solvent: hexane/2-propanol, 80:20; flow: 0.7 mL/min; column: AD Diacel; retention times: *S*, 16.52 min; *R*, 21.21 min]. [c] The absolute configurations were determined by single-crystal X-ray diffraction.

was preferentially obtained; the reaction did not occur at a lower temperature.

In a similar manner to our previous study,^[1a] a PM3 conformational search of diastereoisomeric, zwitterionic, iminium intermediates, resulting from the reaction of the addition of the *anti* or *syn* hydrogen-bonded L-proline acetone enamines to the *Re* and *Si* faces of the keto-carbonyl group of isatin was performed.^[5]

Eight unique lowest-energy conformations were localized and these were used as the starting points for DFT B3LYP/6-311+G** calculations.^[6] The resulting equilibrium geometry (EG) structures were characterized as minima by the lack of any imaginary vibrations (Figure 1, *anti* and *syn* refer to the structure of the enamine, *R* and *S* designate the configuration of the newly formed stereocentre, and the descriptors *cis* and *trans* were used, subjectively, to indicate the position of the proline fragment relative to the aromatic ring of the oxindole fragment). The PM3 EG structures were subsequently used as the starting points for determining PM3 transition-state (TS) geometries of the retro-aldol reaction. These initial PM3 TS structures were then used as inputs for the DFT calculations. From the initial eight inputs, six unique transition states were found and were characterized by a single imaginary frequency that corresponds to the simultaneous formation of the C–C bond and proton transfer from the acid to the forming alkoxide (Figure 1). A seventh transition state (*anti-S-trans*) was located by using a lower level of theory and a single-point calculation was used to determine the energy at a higher level of theory (B3LYP/6-311+G**//B3LYP/6-31G*). After taking into account the necessary corrections, the overall value of $\Delta\Delta G_{298}(\text{TS})$ for this transition state was 7 kcal/mol larger than the lowest-energy transition state and was therefore omitted from Figure 1.

For comparative purposes the corresponding results for the same reaction using 4-bromoisatin as the electrophilic component have been included (Table 2). In the case of the reaction of 4-bromoisatin with the *anti* and *syn* acetone proline enamines, transition states for the structures *Br-anti-R-cis* and *Br-anti-S-cis* were not found, most likely as a consequence of unfavourable steric interactions with the 4-bromo

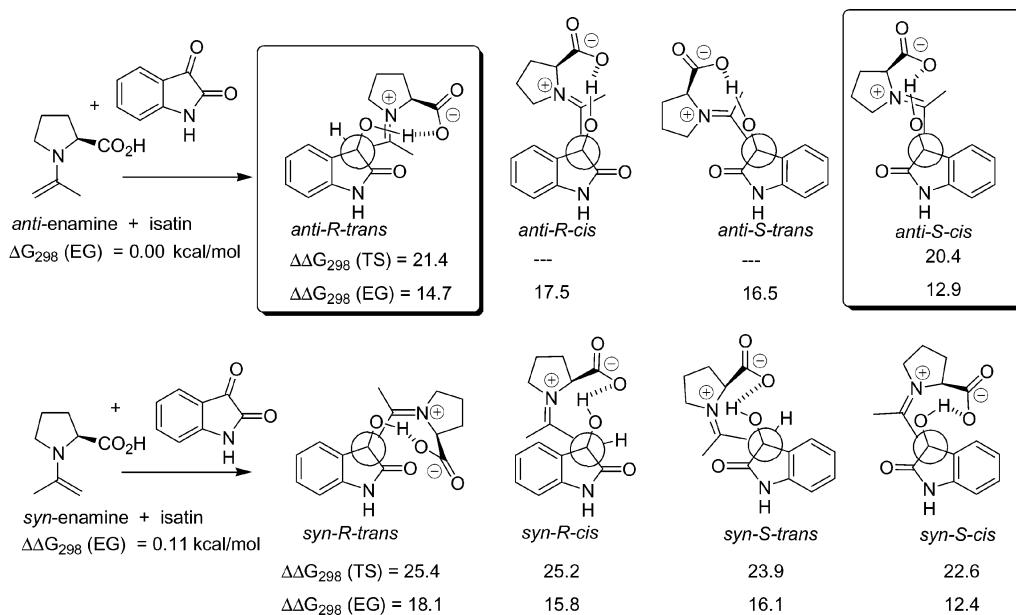


Figure 1. Schematic Newman projections of the eight lowest-energy conformations resulting from the reaction of the *anti* and *syn* acetone L-proline enamines with isatin. The lowest-energy transition states that lead to the formation of the *R* and *S* enantiomers are framed. Hydrogen atoms behind the plane of the oxindole fragment have been omitted for clarity.

Table 2. Relative energies ($\Delta\Delta G_{298}$ [kcal/mol]) for the reaction of the *syn* and *anti* acetone L-proline enamines with 4-bromoisatin (B3LYP/6-311G*).^[a]

<i>anti</i> -Enamine + 4-bromoisatin	<i>Br-anti-R-trans</i>	<i>Br-anti-R-cis</i>	<i>Br-anti-S-trans</i>	<i>Br-anti-S-cis</i>
$\Delta G_{298} = 0$ kcal/mol	$\Delta\Delta G_{298}(\text{TS}) = 17.4$ $\Delta\Delta G_{298}(\text{EG}) = 12.4$	— 17.6	24.5 14.3	— 16.8
<i>syn</i> -Enamine + 4-bromoisatin	<i>Br-syn-R-trans</i>	<i>Br-syn-R-cis</i>	<i>Br-syn-S-trans</i>	<i>Br-syn-S-cis</i>
$\Delta\Delta G_{298} = 0.35$ kcal/mol	$\Delta\Delta G_{298}(\text{TS}) = 25.0$ $\Delta\Delta G_{298}(\text{EG}) = -$	24.5 18.4	21.1 14.2	23.6 15.5

[a] Text printed in **bold** highlights the lowest-energy structures for the formation of the *R* and *S* enantiomers. The acronyms have the same meaning as in Figure 1.

substituent. In addition, the *Br-syn-R-trans* EG structure did not converge.

The DFT results for the addition of the acetone L-proline enamine to isatin are consistent with the experimentally observed result of the preferential formation of the *S* enantiomer (37% *ee* at -15°C). These calculations indicate that the preferred transition states are the *anti-R-trans* and the *anti-S-cis* (see Figures 1 and 2). The value of $\Delta\Delta G^\ddagger$ (1.0 kcal/mol) between these transition states would correspond to an enantiomeric excess much greater than that observed experimentally. This difference may in part be due to solvation effects reducing the energy difference between the transition states in solution.^[4f] Further, the calculated transition states are analogous to the lowest-energy transition states for the reaction of 5,5-dimethylthiazolidine-4-carboxylic acid enamine with benzaldehyde as well as other enamines and aldehydes.^[4g,4h] However, the reaction of isatin with the acetone L-proline enamine differs from the reaction with aldehydes or benzaldehydes in that the isatin reaction passes through an *anti-S-cis* transition state that is lower in energy than the *anti-R-trans* structure.

The equilibrium geometry zwitterionic intermediates obtained in this study and those of our previous study^[1a] as well as those calculated for the aldol reaction with benzaldehyde (see below) reveal unusually large C–C(O₂) bond lengths (1.60–1.64 Å). However, these zwitterionic intermediates are stabilized by an internal hydrogen bond with the tertiary alcohol. The importance of the hydrogen bond for the stability of the zwitterionic intermediates was tested by intentionally disrupting the hydrogen-bonding. This resulted in the decarboxylation of the zwitterionic intermediate to give an azomethine ylide. Such species are known to be generated in the reaction of amino acids with carbonyl compounds via unstable oxazolidinone intermediates.^[7] However, in a number of instances oxazolidinones are known to be stable, isolable intermediates and it has been recently suggested that oxazolidinones may play a central role in the cross-aldol reaction.^[8] Therefore, in order to investigate the possibility that oxazolidinones may be intermediates along the reaction coordinate, and that they may possibly influence the stereochemical outcome, their structures were calculated. Indeed, oxazolidinones [(*R*)-5 EG

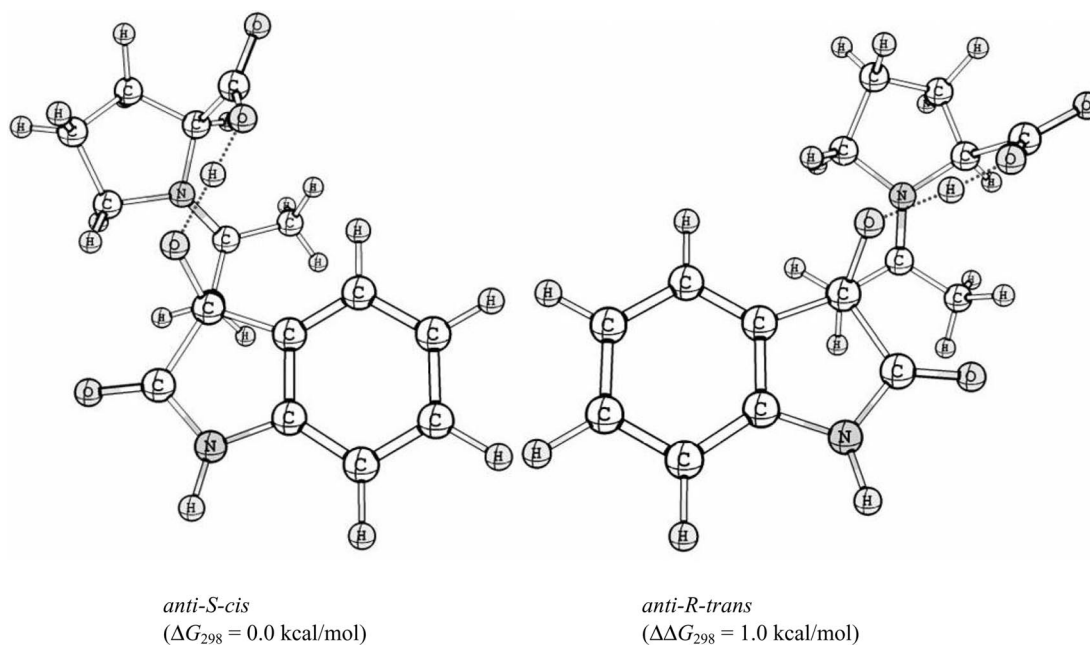


Figure 2. The lowest-energy transition states for the formation of the *S* and *R* enantiomers for the reaction of L-proline enamine with isatin.

and (*S*)-**5** EG] were readily found to be minima on the reaction coordinate and (*R*)-**5** EG is more stable than (*S*)-**5** EG ($\Delta G = 0.4$ kcal/mol) (see Figures 3 and 4). The transition states for the ring-opening of these oxazolidinones were readily located and found to be marginally lower (0.4 kcal/mol) in energy in the case of the (*S*)-**5** TS and slightly higher (0.9 kcal/mol) in the case of the (*R*)-**5** TS ($\Delta\Delta G^\ddagger = 2.3$ kcal/mol) with respect to the cross-aldol transition states (Figure 4). In addition to the reaction paths crossing from the cross-aldol TS to the oxazolidinone intermediates, it was found that the corresponding transition states for the ring-opening of the oxazolidinones also crossed such that ring-opening of the (*R*)-**5** EG passed through the higher-energy transition state. According to the calculated energies of the transition states and intermediates (Figure 3), as there is sufficient thermal energy for product formation even at temperatures substantially below room temperature and the activation barrier for the cross-aldol step is greater than that for the oxazolidinone ring-opening, the $\Delta\Delta G^\ddagger$ for the cross-aldol reaction would control the enantioselectivity by kinetic control. However, if the cross-aldol reaction step was reversible then the overall enantioselectivity could be modified by subsequent steps in the reaction mechanism.

In this case the participation of the oxazolidinones (*R*)-**5** and (*S*)-**5** would result in an even greater selectivity for the formation of the *S* enantiomer as a consequence of a change in the reaction step of highest activation energy for each enantiomer [$\Delta\Delta G^\ddagger = \Delta G^\ddagger[(R)\text{-}5\text{ TS}] - \Delta G^\ddagger[\text{anti-}S\text{-cis TS}]$]. Therefore at this point it seems unlikely that **5** influences the stereoselectivity of the cross-aldol reaction.

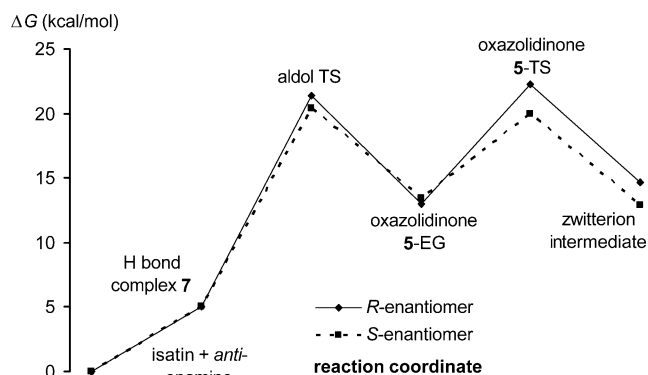


Figure 4. Reaction coordinate for the cross-aldol addition of acetone to isatin.

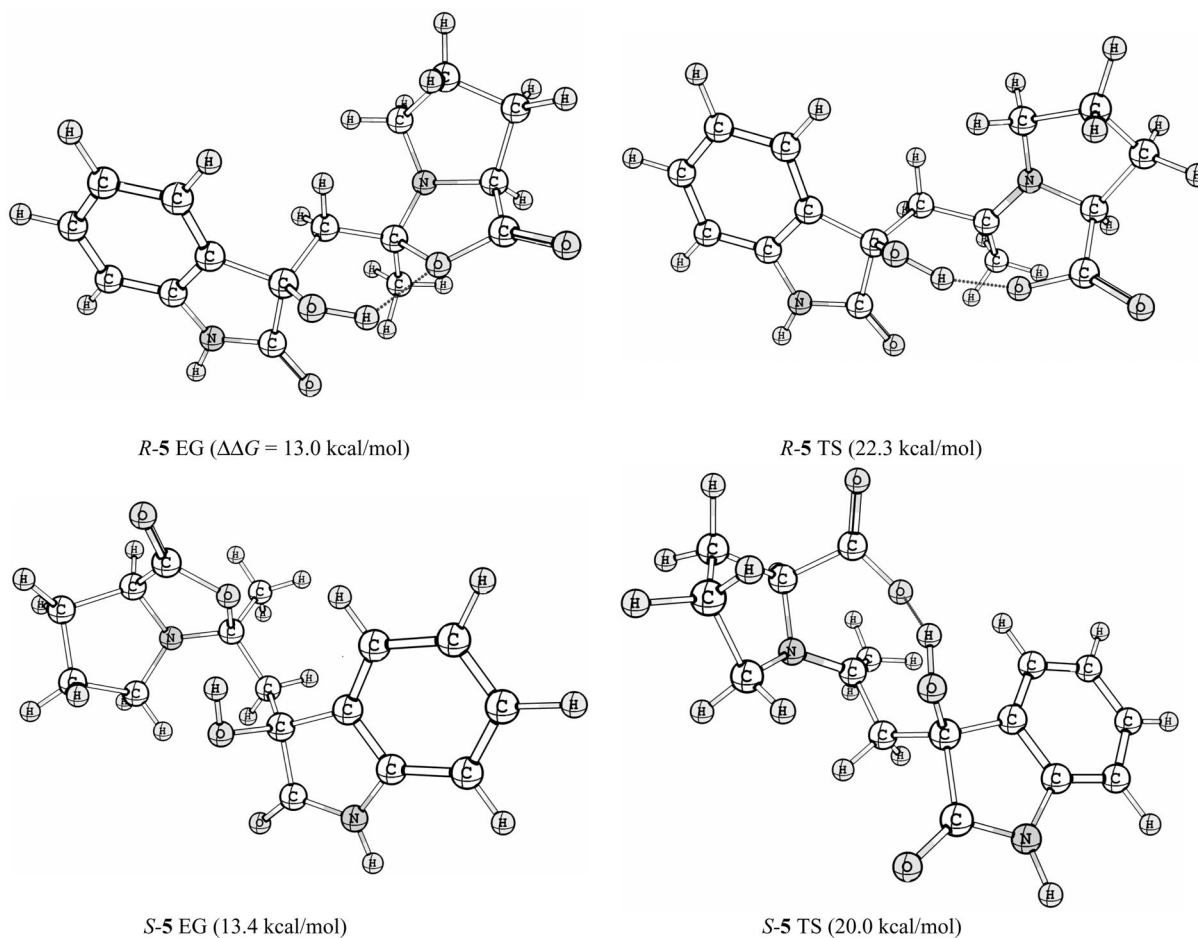


Figure 3. Structures of (*R*)- and (*S*)-oxazolidinone (**5**) equilibrium geometries (EG) and the corresponding ring-opening transition states (TS). The values of $\Delta\Delta G$ are cited relative to isatin and to the *anti*-enamine derived from proline and acetone.

The *anti-S-cis* and *anti-R-trans* cross-aldol transition states described in Figure 2 have certain similarities as they both have staggered conformations around the forming C...C bond with C–C(enamine)···C–O(keto-carbonyl) dihedral angles of 39.6 and 41.4°, respectively. The C...C bond lengths are 1.84 and 1.78 Å and the angles for O–C...C are 111.2 and 111.3°, respectively. For both transition states the only evident steric interaction arises between the methyl group of the enamine and either the aromatic ring (*anti-S-cis*, H...H closest contact 2.56 Å) or the amide carbonyl group (*anti-R-trans*). This steric interaction is equivalent to the 1,3-diaxial interaction invoked in Zimmerman–Traxler transition states for the aldol reaction of metal enolates.^[9] For the *anti-R-trans* TS, the proximity of the methyl hydrogen atoms and the carbonyl oxygen (H...O closest contact 2.55 Å) could potentially result in an electrostatic interaction of the type $\delta^- \text{O} \cdots \text{CH}_3^{\delta+} \text{C}=\text{N}$. These secondary interactions have been suggested to have a stabilizing effect.^[4g,10] However, in this case, given the distance separating the groups and the fact that the *anti-R-trans* TS is of greater energy, it would seem reasonable to conclude that no such stabilizing interaction is present. From an AIM study (see below) two further electrostatic interactions could be discerned: the interactions between the forming alkoxide oxygen (δ^-) and (i) the pyrrolidine nitrogen atom (more or less neutral) and (ii) the $\alpha\text{-CH}_2$ of the pyrrolidine ring. However, the distances involved for both the *anti-S-cis* and the *anti-R-trans* transition states would indicate that these electrostatic interactions are of minimal importance (see Table 4).

The prevailing structural difference between the two transition states involves a nucleophilic attack of the enamine $\text{CH}_2=\text{C}(\text{N})$ on the keto-carbonyl group in a manner such that the enamine $\text{CH}_2=\text{C}(\text{N})$ bond is either antiperiplanar to the $\text{C}_{\text{keto}}\text{--C}_{\text{amide}}$ (*anti-S-cis*) or $\text{C}_{\text{keto}}\text{--C}_{\text{aryl}}$ (*anti-R-trans*) bond. These transition states result in dipole moments of 6.79 and 8.96 D, respectively. The calculated dipole moments for the transition states are in accord with the preference for the formation of the *S* enantiomer in the gas phase. However, the transition state *syn-S-cis* has the smallest dipole moment of all the structures (6.72 D) but it is higher in energy than the two lowest-energy transition states (Figure 1). Therefore, minimization of the dipole moment does not offer a complete explanation for the preferential formation of the *S* enantiomer. Given the different electronic natures of the aforementioned C–C bonds, it is possible that in the case of isatin, in which there is no voluminous substituent on the 4-position of the aromatic ring, that a subtle stereoelectronic effect may be responsible for controlling the inversion of the stereochemistry in comparison to the related reaction with aldehydes.^[4] The $\text{C}_{\text{keto}}\text{--C}_{\text{amide}}$ bond of isatin would be expected to be relatively deficient in electron density due to the electronic nature of the carbonyl groups. Indeed, earlier studies have questioned the nature of the $\text{C}_{\text{keto}}\text{--C}_{\text{amide}}$ bond in isatin due to it being relatively long (1.555 Å).^[11] It was initially considered that the long bond length was a consequence of electron-pair repulsion between the carbonyl oxygen atoms. However,

such long bond lengths are found in both *cis*- and *trans*-1,2-dicarbonyl systems that are not constrained within a ring and therefore electron-pair repulsion cannot be responsible for the observed bond length.^[12] The long C–C bond lengths were attributed to the electronegativity of the oxygen atoms that results in a repulsive interaction between the partially positively charged carbon atoms of the $\text{C}(\text{O})\text{--C}(\text{O})$ bond. In addition, it was proposed that a negative hyperconjugative interaction between the oxygen lone-pairs and the σ^* C–C bond orbital would lead to lengthening of the central C–C bond in isatin.^[12] A molecular orbital analysis reveals that in an antiperiplanar arrangement the HOMO of the enamine could equally well overlap with the LUMO of isatin either on the *Re* face to give the *anti-R-trans* TS or on the *Si* face to give the *anti-S-cis* TS.

With the intention of further investigating the possible influence of the antiperiplanar nature of the C–C bond with respect to the enamine double bond, a comparison of the two lowest-energy transition states for the cross-aldol reaction of isatin and acetone was made with that of benzaldehyde and acetone. The latter was calculated in this study at the B3LYP/6-311+G**//B3LYP/6-31G* level of theory and the results are presented in Table 3.

Table 3. ChelpG charges of the atoms in the carboxylate ($\text{O}^1=\text{C}\text{--}\text{O}^{2\cdots}\text{H}\cdots\text{O}_{\text{keto}}\text{--C}_{\text{keto}}\text{--C}_{\text{aryl}}$), $\text{O}_{\text{amide}}=\text{C}_{\text{amide}}$ and enamine ($\text{N}\text{--C}_{\alpha}=\text{C}_{\beta}$) fragments.

	<i>anti-R-trans</i>	<i>anti-S-cis</i>	<i>ben-R</i>	<i>ben-S</i>
O^1	–0.625	–0.646	–0.637	–0.639
C	0.891	0.953	0.892	0.873
O^2	–0.693	–0.776	–0.759	–0.716
H	0.522	0.603	0.576	0.594
O_{keto}	–0.814	–0.878	–0.776	–0.850
C_{keto}	0.501	0.654	0.451	0.592
C_{aryl}	–0.145	–0.227	0.082	–0.061
C_{amide}	0.716	0.696	–0.047 ^[a]	–0.042 ^[a]
O_{amide}	–0.596	–0.580	–	–
N	–0.058	–0.081	–0.006	0.009
C_{α}	0.300	0.201	0.184	0.089
C_{β}	–0.255	–0.285	–0.208	–0.182
Residual charge ^[b]	–0.416	–0.385	–0.362	–0.380

[a] ChelpG charge of the hydrogen atom of the aldehyde group. [b] Sum of the ChelpG charges over all the atoms in the electrophile.

The ChelpG charges of the carboxylate $\text{O}^1=\text{C}\text{--}\text{O}^{2\cdots}\text{H}\cdots\text{O}_{\text{keto}}\text{--C}_{\text{keto}}\text{--C}_{\text{aryl}}$ and the enamine $\text{N}\text{--C}_{\alpha}=\text{C}_{\beta}$ (principally the central carbon, C_{α}) fragments of the *anti-S-cis* and *anti-R-trans* transition states for isatin and the corresponding fragments for the *ben-R* and *ben-S* transition states for benzaldehyde reveal large differences between the diastereomeric transition states. However, in general terms the same trend in changes in charge is observed when comparing *anti-R-trans* with *anti-S-cis* for isatin and for *ben-R* with *ben-S* for benzaldehyde (where *ben-R* and *ben-S* are, respectively, the transition states for the reactions of benzaldehyde with the acetone proline enamine that result in the formation of the *R* and *S* cross-aldol product enantiomers). Owing to this similarity it can be concluded that the distribution of charge does not control the lowest-energy transition state.

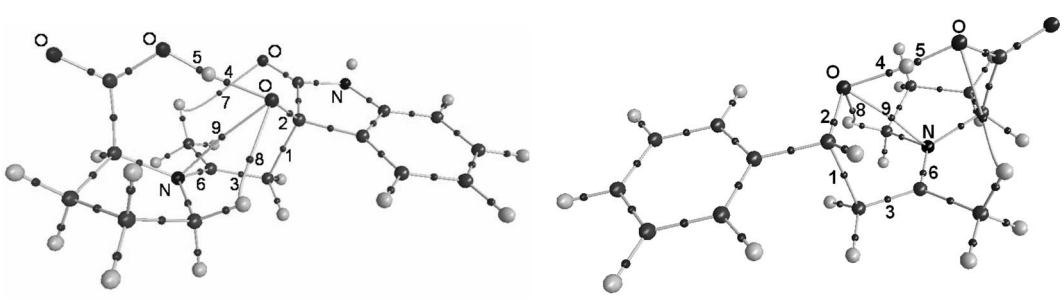
Furthermore, by comparing the ChelpG charges it can be seen that there is a lesser residual charge associated with the electrophile for the lower-energy transition states of the reactions involving isatin and benzaldehyde. This result can be associated with the longer-forming C...C bonds and the greater degree of proton transfer (Table 4) in the lower-energy transition states, thus resulting in a lower energetic cost associated with a lower overall difference in charge redistribution on the electrophile.

The possibility of a stereoelectronic effect was also investigated by using AIM theory.^[13,14] In AIM theory, the interaction between two atoms is revealed by the presence of a charge density in the interconnecting space and this charge density is related to a bond critical point (BCP). Therefore, AIM can be used to infer the existence, or otherwise, of a molecular interaction.^[15] With the objective of comparing the two lowest-energy transition states for the cross-aldol reaction of isatin and acetone with those of the cross-aldol reaction of benzaldehyde with acetone, Table 4 lists selected BCPs and the corresponding bond lengths for these transition states. It is immediately clear that for both reactions the lower-energy transition state has the longer-forming C...C bond (BCP 1) and that the forming C...C bonds are shorter for isatin than for benzaldehyde. The only other notable difference between the reactions involving isatin and benzaldehyde is the degree of transfer of the proton from the carboxylic acid to the forming alkoxide anion (BCPs 4 and 5). In the case of the reaction with benzaldehyde, the transfer of the proton is marginally less advanced in the lower-energy transition state.

However, the corresponding transition states for the reaction of isatin reveal that the proton has been transferred to a greater degree in the lower-energy transition state than in the higher-energy transition state and further, that the proton has been transferred to a lesser degree than in the case of the benzaldehyde reaction. Further comparison of the degree of transfer of the proton reveals that the proton is consistently less transferred in the analogous transition states: *anti-R-trans* and *ben-R*, and vice versa for the transition states that ultimately lead to the *S* enantiomer (*anti-S-cis* and *ben-S*). Secondary electrostatic interactions^[4g,10] (BCPs 7, 8 and 9) are negligible and no interaction between the transferring proton with the enamine nitrogen is observed. Analysis of the BCPs and bond lengths associated with the heterocyclic oxindole ring (not shown in Table 4) reveal that the bonds are essentially equivalent in both the *anti-S-cis* and the *anti-R-trans* transition states.

Finally, owing to the observed differences in the degree of proton transfer it seemed reasonable to question whether or not there was an energy difference involved in the formation of a hydrogen bond with either of the keto-carbonyl group lone-pairs. In order to investigate this, two approaches were taken: first, the problem was simplified by calculating the energy of the hydrogen-bonded complex formed between isatin and a water molecule, and secondly, attempts were made to locate hydrogen-bonded complexes of the acetone proline enamine and isatin formed on the inside and outside lone-pair electrons of the keto-carbonyl group (where the inside and outside are defined as being *cis* to the amide carbonyl or *cis* to the aryl ring, respectively).

Table 4. AIM data for the bond critical points and the corresponding bond lengths associated with the lowest-energy transition states for the reactions of isatin and benzaldehyde with the acetone proline enamine.



		<i>anti-R-trans</i> TS			<i>ben-R</i> TS					
Structure		1	2	3	Bond critical point (BCP)			7	8	9
					4	5	6			
<i>anti-R-trans</i>	ρ [a.u.] ^[a]	0.140	0.336	0.282	0.087	0.260	0.342	0.010	0.015	0.017
	d [Å] ^[b]	1.782	1.307	1.445	1.442	1.057	1.315	2.546	2.326	2.763
<i>anti-S-cis</i>	ρ [a.u.] ^[a]	0.124	0.338	0.288	0.106	0.239	0.342	0.004 ^[c]	0.015	0.018
	d [Å] ^[b]	1.838	1.303	1.433	1.371	1.086	1.317	2.558 ^[c]	2.338	2.717
<i>ben-R</i>	ρ [a.u.] ^[a]	0.111	0.336	0.293	0.115	0.226	0.336	—	0.014	0.016
	d [Å] ^[b]	1.883	1.304	1.423	1.352	1.104	1.325	—	2.370	2.785
<i>ben-S</i>	ρ [a.u.] ^[a]	0.117	0.332	0.291	0.118	0.219	0.337	—	0.015	0.016
	d [Å] ^[b]	1.861	1.309	1.427	1.337	1.115	1.323	—	2.339	2.784

[a] Charge density (ρ) associated with the corresponding interaction between two atoms. BCPs 7, 8 and 9 reveal secondary electrostatic interactions. [b] Bond lengths for each BCP. [c] BCP 7 corresponds to the interaction of the methyl group with 4-H of the oxindole nucleus.

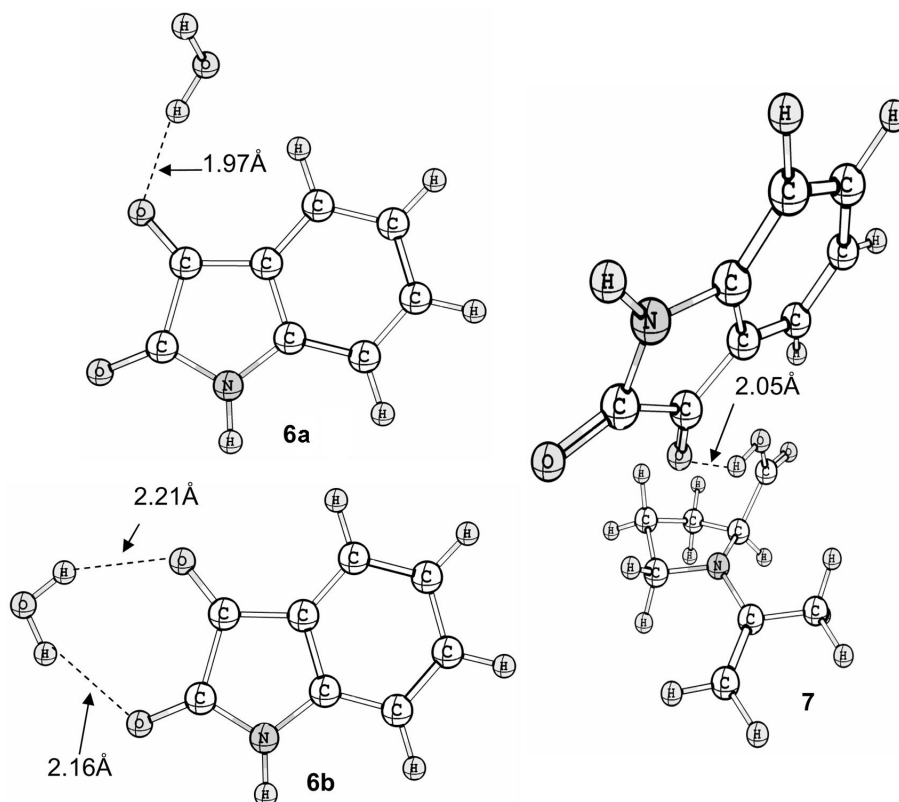


Figure 5. Hydrogen-bonded complexes: water hydrogen-bonded to a) the outside lone-pair (**6a**) and b) the inside lone-pairs (**6b**). c) Isatin and the *anti*-acetone proline enamine (**7**).

The first method revealed a preference for water to be hydrogen-bonded to the outside lone-pair of the keto-carbonyl group for which the difference in energy between the two isomeric structures (**6a** vs. **6b**, Figure 5) is very similar (1.3 kcal/mol) to that found for the two isomeric transition states (*anti-R-trans* and *anti-S-cis*). An AIM analysis of the hydrogen-bonded complexes **6a** and **6b** was consistent with the favoured hydrogen-bonding to the outside lone-pair ($\rho = 0.0256$ a.u.), as revealed by a ρ value approximately twice as large as that for the complex involving a hydrogen bond to the inside lone-pair ($\rho = 0.0149$ a.u.). In both complexes the negative values of the Laplacian revealed that the charge density is concentrated along the bond path, where once again a more negative value was obtained for the outside hydrogen-bonded complex. The second approach is relatively more complex and was initially modelled by using the PM3 method. Interestingly, all attempts to backtrack the *anti-R-trans* TS to a hydrogen-bonded complex resulted in the same structure as that obtained for a similar process involving the *anti-S-cis* TS. This structure was subsequently optimized by DFT. The resulting complex **7** involves a hydrogen bond from the enamine to the outside lone-pair of isatin (Figure 5). The preferred hydrogen-bonding to the outside lone-pair involves donation of the lone pair to the anti-bonding σ^* of the O–H bond and at the same time avoids an unfavourable electrostatic interaction between the electronegative oxygen of the amide group and of the carboxylic acid group. In the case of **6b** this unfavourable inter-

action is avoided by water simultaneously hydrogen-bonding to both carbonyl groups. The complex **7** is interesting as it can be envisioned that a simple clockwise rotation around the hydrogen bond will result in a conformation that resembles the lowest-energy *anti-S-cis* TS. Although an anticlockwise rotation would give an *anti-R-cis* conformation, a further rotation around an axis between the reactive carbon centres would be required to give the *anti-R-trans* conformation. Thus, for substrates to pass through the *anti-R-trans* TS there is a larger energetic cost associated with a greater degree of structural reorganization in comparison to the reaction passing through the *anti-S-cis* TS conformation.

In light of the results obtained in this study for the reaction of L-proline enamine with isatin, the results for the calculations of the reaction of 4-bromoisatin can be more fully appreciated. In the case of the reaction with 4-bromoisatin, the bromo substituent causes a steric interaction with either the pyrrolidine ring or with the methyl group of the enamine thus impeding the reaction via the *Br-anti-R-cis* or *Br-anti-S-cis* conformers (the corresponding TSs could not be localized by using DFT)^[1a] or resulting in higher-energy transition states for the reaction of the *syn* enamine with the exception of the *Br-syn-S-trans* TS in which the interaction with the 4-bromo substituent is minimized by the proline enamine being rotated away from the 4-bromo substituent.

Therefore the introduction of a large substituent at the 4-position of the aromatic ring is sufficient to sterically

overcome the stereoelectronic effect observed in the unsubstituted system, but at the same time the reaction of 4-bromoisatin does not follow a similar reaction manifold to benzaldehyde, or other aldehydes, as a consequence of steric hindrance in the formation of the *anti-S-cis* transition state (reaction by addition of the *anti*-enamine to the *Re* and *Si* faces in an antiperiplanar manner to the C_{aldehyde}–C_{aromatic} bond and the C_{hydrogen}–C_{aldehyde} bonds in accord with transition states for aldehydes).

Finally, the calculated reaction of isatin reveals that the formation of the post-aldol iminium intermediate is endothermic, as previously observed for the calculated reaction of 4-bromoisatin. Therefore, the aldol reaction could be reversible depending upon the energetics of the hydrolysis reaction. If the transition states for the hydrolysis reaction are higher in energy than the aldol transition states, then the enantiomeric excess could be determined either by the difference in activation energy for the hydrolysis reaction or by the equilibrium constant for formation of an intermediate followed by the subsequent rates for hydrolysis.

Conclusions

We have studied by means of DFT and AIM calculations the steric and stereoelectronic effects that control the enantioselectivity in the cross-aldol addition of acetone to isatin catalyzed by L-proline. This reaction gives smaller enantiomeric excesses and a reversal of enantioselectivity in comparison with the corresponding addition to 4,6-dibromoisatin.

DFT calculations of the cross-aldol transition states indicate that product formation follows different pathways for isatin and 4,6-dibromoisatin. In the case of isatin, the *S* enantiomer is favoured as a consequence of a stereoelectronic effect that reverses the transition-state energies of the *S* and *R* enantiomers relative to the proposed transition states for the cross-aldol addition to aldehydes. In contrast, the cross-aldol addition of acetone to 4,6-dibromoisatin furnishes the expected *R* enantiomer owing to the steric effect of the 4-bromo substituent which inhibits the formation of the stereoelectronically preferred transition state for the formation of the *S* enantiomer. In aldehydes, the observed enantioselectivity is a consequence of the minimization of steric interactions, whereas in reactive ketones, such as isatin, the observed selectivity is a consequence of a preferential stereoelectronic protonation of the keto-carbonyl group.

Experimental Section

General Method for the Synthesis of 3-(2-Oxopropyl)-3-hydroxyindolin-2-ones: L-Proline (0.03 mmol, 3.5 mg) was stirred in acetone (2 mL) for 15 min at the temperature described in Table 1. Solid isatin (0.3 mmol, 44 mg) or 4,6-dibromoisatin (0.3 mmol, 91 mg) was added and the mixture was stirred for 17 h. After this time acetone was removed under reduced pressure and the mixture was purified by flash chromatography (cyclohexane/ethyl acetate, 1:1) to eliminate the catalyst. The enantiomeric excesses were determined by chiral HPLC of the crude. Analytical high-performance

liquid chromatography (HPLC) was performed on a HP 1090 liquid chromatograph equipped with a variable-wavelength UV detector (deuterium lamp 190–600 nm) using a Daicel CHIRALPAK® AD column (0.46×25 cm) (Daicel Inc.). Conditions: (i) for R = H: solvent: hexane/2-propanol, 80:20; flow: 0.9 mL/min; retention times, *S*: 11.66 min; *R*: 15.28 min; (ii) for R = Br: solvent: hexane/2-propanol, 80:20; flow: 0.7 mL/min; retention times, *S*: 16.52 min; *R*: 21.21 min. Characterization of the reaction products has been described previously.^[1]

Theoretical Calculations: The methodology for the obtainment of the structures for the DFT calculations has been previously detailed.^[1a] All PM3 calculations were performed by using Spartan 02^[5] whereas all the DFT (B3LYP) calculations were performed by using Gaussian 98.^[6] In our previous study the basis set was limited to 6-311G* due to use of the lanl2dz basis set for the description of the bromine atom. In this study we included a diffuse function and an additional polarization function in the basis set (6-311+G**) with the objective of obtaining better absolute energies and geometries. The (*R*)- and (*S*)-5 EG structures were initially obtained by using a PM3 conformational search as implemented in Spartan 02.^[5] These structures were subsequently employed as starting points for the PM3 calculation of the ring-opening transition states to give the (*R*)- and (*S*)-5 TS structures. The lowest-energy PM3 (*R*)- and (*S*)-5 EG and TS structures were used as starting points for the DFT calculations. The isatin/water hydrogen-bonded structures **6a** and **6b** were initially calculated by using PM3 and then subjected to DFT B3LYP calculations. For complex **7**, the PM3 *anti-R-trans* and *anti-S-cis* transition states were reverted to substrates by the initial use of a distance constraint for the forming C···C bond and optimized by PM3 so as to give greater substrate character to the complex. Subsequently, the complexes were subjected to equilibrium geometry PM3 optimization with no constraints. Irrespective of the structure of the transition state initially used, the lowest-energy conformer always formed a hydrogen bond to the outside lone-pair. This structure was used as the input for the DFT B3LYP calculation.

Acknowledgments

G. A. and C. T. thank the Ministero dell'Università e della Ricerca (MIUR) (PRIN 2006 "Sintesi, attività biologica e applicazioni diagnostiche di ligandi delle integrine α -v- β -3, α -4- β -1 e α -4- β -7") and the University of Bologna (Funds for selected topics) for financial support. S. J. G. thanks the Brazilian Conselho Nacional de Desenvolvimento Científico e Tecnológico (CNPq) for financial support (Grant process 302270/2004-3).

- [1] a) G. Luppi, M. Monari, R. J. Corrêa, F. de A. Violante, A. C. Pinto, B. Kaptein, Q. B. Broxterman, S. J. Garden, C. Tomasini, *Tetrahedron* **2006**, 62, 12017–12024; b) G. Luppi, P. G. Cozzi, M. Monari, B. Kaptein, Q. B. Broxterman, C. Tomasini, *J. Org. Chem.* **2005**, 70, 7418–7421.
- [2] For reviews on the synthesis of quaternary carbon centres, see: a) C. Cativiela, M. D. Diaz-de-Villegas, *Tetrahedron: Asymmetry* **2007**, 18, 569–623; b) J. Christoffers, A. Baro (Eds.), *Quaternary Stereocenters*, Wiley-VCH, Weinheim, **2005**; c) C. J. Douglas, L. E. Overman, *Proc. Natl. Acad. Sci. USA* **2004**, 101, 5363–5367; d) I. Denissova, L. Barriault, *Tetrahedron* **2003**, 59, 10105–10146; e) J. Christoffers, A. Mann, *Angew. Chem. Int. Ed.* **2001**, 40, 4591–4597; f) E. J. Corey, A. Guzman-Perez, *Angew. Chem. Int. Ed.* **1998**, 37, 388–401; g) K. Fuji, *Chem. Rev.* **1993**, 93, 2037–2066; h) S. F. Martin, *Tetrahedron* **1980**, 36, 419–460.

- [3] a) H.-p. Zhang, H. Shigemori, M. Ishibashi, T. Kosaka, G. R. Pettit, Y. Kamano, J. Kobayashi, *Tetrahedron* **1994**, *50*, 10201–10206; b) Y. Kamano, H.-p. Zhang, Y. Ichihara, H. Kizu, K. Komiyama, G. R. Pettit, *Tetrahedron Lett.* **1995**, *36*, 2783–2784; c) Y. Kamano, H.-p. Zhang, Y. Ichihara, H. Kizu, K. Komiyama, G. R. Pettit, *Tetrahedron Lett.* **1995**, *36*, 2783–2784; d) T. Kawasaki, M. Nagaoka, T. Satoh, A. Okamoto, R. Ukon, A. Ogawa, *Tetrahedron* **2004**, *60*, 3493–3503; e) S. J. Garden, J. C. Torres, A. Ferreira, R. B. Silva, A. C. Pinto, *Tetrahedron Lett.* **1997**, *38*, 1501–1504; f) G. K. Jnaneshwar, A. V. Bedekar, V. H. Deshpande, *Synth. Commun.* **1999**, *29*, 3627–3633; g) G. K. Jnaneshwar, V. H. J. Deshpande, *Chem. Res. (S)* **1999**, 632–633; h) T. Nakamura, S.-i. Shirokawa, S. Hosokawa, A. Nakazaki, S. Kobayashi, *Org. Lett.* **2006**, *8*, 677–679; i) G. Cravotto, G. B. Giovenzana, G. Palmisano, A. Penoni, T. Pilati, M. Sisti, F. Stazi, *Tetrahedron: Asymmetry* **2006**, *17*, 3070–3074.
- [4] a) B. List, R. A. Lerner, C. F. Barbas III, *J. Am. Chem. Soc.* **2000**, *122*, 2395–2396; b) W. Notz, B. List, *J. Am. Chem. Soc.* **2000**, *122*, 7386–7387; c) K. Sakthivel, W. Notz, T. Bui, C. F. Barbas, *J. Am. Chem. Soc.* **2001**, *123*, 5260–5267; d) B. List, *Synlett* **2001**, 1675–1686; e) A. Córdova, W. Notz, C. F. Barbas III, *J. Org. Chem.* **2002**, *67*, 301–303; f) K. N. Rankin, J. W. Gault, R. J. Boyd, *J. Phys. Chem. A* **2002**, *106*, 5155–5159; g) S. Bahmanyar, K. N. Houk, H. J. Martin, B. List, *J. Am. Chem. Soc.* **2003**, *125*, 2475–2479; h) C. Allemann, R. Gordillo, F. R. Clemente, P. H. Y. Cheong, K. N. Houk, *Acc. Chem. Res.* **2004**, *37*, 558–569; i) W. Notz, F. Tanaka, C. F. Barbas III, *Acc. Chem. Res.* **2004**, *37*, 580–591.
- [5] All PM3 calculations were performed using *Spartan 02*, Wavefunction, Inc., Irvine, CA.
- [6] Calculations were performed at the B3LYP/6-311+G** level of theory for C, H, N and O atoms. M. J. Frisch, G. W. Trucks, H. B. Schlegel, G. E. Scuseria, M. A. Robb, J. R. Cheeseman, V. G. Zakrzewski, J. A. Montgomery, Jr., R. E. Stratmann, J. C. Burant, S. Dapprich, J. M. Millam, A. D. Daniels, K. N. Kudin, M. C. Strain, O. Farkas, J. Tomasi, V. Barone, M. Cossi, R. Cammi, B. Mennucci, C. Pomelli, C. Adamo, S. Clifford, J. Ochterski, G. A. Petersson, P. Y. Ayala, Q. Cui, K. Morokuma, D. K. Malick, A. D. Rabuck, K. Raghavachari, J. B. Foresman, J. Cioslowski, J. V. Ortiz, A. G. Baboul, B. B. Stefanov, G. Liu, A. Liashenko, P. Piskorz, I. Komaromi, R. Gomperts, R. L. Martin, D. J. Fox, T. Keith, M. A. Al-Laham, C. Y. Peng, A. Nanayakkara, C. Gonzalez, M. Challacombe, P. M. W. Gill, B. G. Johnson, W. Chen, M. W. Wong, J. L. Andres, M. Head-Gordon, E. S. Replogle, J. A. Pople, *Gaussian 98*, revision A.7, Gaussian, Inc., Pittsburgh, PA, **1998**.
- [7] a) R. Grigg, J. Idle, P. McMeekin, S. Surendrakumar, D. Vipond, *J. Chem. Soc. Perkin Trans. 1* **1988**, 2703–2713; b) M. F. Aly, R. Grigg, S. Thianpatanagul, V. Sridharan, *J. Chem. Soc. Perkin Trans. 1* **1988**, 949–955; c) R. Grigg, J. Idle, P. McMeekin, D. Vipond, *J. Chem. Soc. Chem. Commun.* **1987**, 49–51.
- [8] D. Seebach, A. K. Beck, D. M. Badine, M. Limbach, A. Eschenmoser, A. M. Treasurywala, R. Hobi, W. Prikoszovich, B. Linder, *Helv. Chim. Acta* **2007**, *90*, 425–471.
- [9] H. E. Zimmerman, M. D. Traxler, *J. Am. Chem. Soc.* **1957**, *79*, 1920–1923.
- [10] C. E. Cannizzaro, K. N. Houk, *J. Am. Chem. Soc.* **2002**, *124*, 7163–7169.
- [11] G. J. Palenik, A. E. Koziol, A. R. Katritzky, W.-Q. Fan, *J. Chem. Soc. Chem. Commun.* **1990**, 715–716.
- [12] A. Rathna, J. Chandrasekhar, *J. Chem. Soc. Perkin Trans. 2* **1991**, 1661–1666.
- [13] All calculations were performed using the AIM2000 program, v2.0, and were based upon wavefunctions calculated at the B3LYP/6-311+G** level of theory: F. Biegler-König, J. Schönbohm, D. Bayles, *J. Comput. Chem.* **2001**, *22*, 545–559.
- [14] For a recent example of the use of AIM to investigate stereo-electronic effects, see: H. Roohi, A. Ebrahimi, S. M. Habibi, E. Jarahi, *THEOCHEM* **2006**, *772*, 65–73.
- [15] R. F. W. Bader, *Atoms in Molecules. A Quantum Theory*, Clarendon Press, Oxford, **1990**.

Received: October 5, 2007

Published Online: December 3, 2007